Superconductivity at the Normal Metal/Dirac Semimetal Cd_3As_2 Interface

Shuai Zhang(张帅)[1*], Yiyan Wang(王义炎)[1,2], Chaoyang Ma(麻朝阳)[1], Wenliang Zhu(朱文亮)[1,2], Zhian Ren(任治安)[1,2,3], Lei Shan(单磊)[4*], and Genfu Chen(陈根富)[1,2,3*]

[1]*Institute of Physics and Beijing National Laboratory for Condensed Matter Physics, Chinese Academy of Sciences, Beijing 100190, China*

[2]*School of Physical Sciences, University of Chinese Academy of Sciences, Beijing 100049, China*

[3]*Songshan Lake Materials Laboratory, Dongguan 523808, China*

[4]*Key Laboratory of Structure and Functional Regulation of Hybrid Materials of Ministry of Education, Institutes of Physical Science and Information Technology, Anhui University, Hefei 230601, China*

(Received 26 April 2020; accepted 20 May 2020; published online 21 June 2020)

We investigate the interface between a three-dimensional Dirac semimetal Cd_3As_2 and a normal metal via soft-point contact spectroscopy measurement. The superconducting gap features were detected below 3.8 K and 7.1 K in the case of Cd_3As_2 single crystals sputter-coated with the Pt and Au films, respectively, in the differential conductance dI/dV–V plots of the point contacts. As the applied magnetic field increased, the drop in the zero-bias contact resistance shifted toward lower temperatures. The topologically non-trivial band structure of Cd_3As_2 is considered to play a crucial role in inducing the superconductivity. Apart from realizing superconductivity in topological materials, our creative approach can be used to investigate possible topological superconductivity and exhibits a high application potential in electronic devices.

PACS: 74.78.−w, 74.70.−b, 74.25.Sv DOI: 10.1088/0256-307X/37/7/077401

Recently, superconductivity has been induced at the hard point contact (PC) between a normal metal tip and the topological materials such as the three-dimensional (3D) Dirac semimetal Cd_3As_2,[1] the Weyl semimetals TaAs[2,3] and WC,[4] and the nodal-line semimetal ZrSiS.[5] The unconventional natures of these tip-induced superconductivity has been reported simultaneously, suggesting a potential route to achieve topological superconductivity.[6] Most of these induced superconducting phenomena are interpreted as nanometer-scale junctions between the non-superconducting tip metals (such as Fe, Co, Ni, Ag, Au and Pt) and the crystal surface, causing explicit symmetry breaking. Importantly, the coexistence of the emerging tip-induced superconducting phase and the well-preserved topological properties of ZrSiS suggest an evolution from the topological to a superconducting state.[5] Alternatively, the local pressure around the tip contact could become sufficiently high to cause band reconstruction, a confinement effect, and charge carrier doping, all of which subsequently contribute to the emergence of the superconductivity. Because pressure-induced superconductivity has not been observed in bulk crystals, this scenario remains open to debate.

In general, the absence of superconducting behavior when using the soft PC method could support the scenario of tip pressure-induced superconductivity.[1] Recently, our group achieved interfacial superconductivity between a thin metal film and the topological materials of TaAs and WC, with superconducting transitions up to 3.2 and 11.5 K,[7] respectively. Furthermore, although a zero resistance has not yet been realized, the superconducting transition of Ag-deposited TaAs single crystals is accompanied by a drop in the resistance $R(T)$, as measured using the traditional four-point-probe resistivity measurements. In this letter, we report the detection of superconductivity at the Au(Pt)/Cd_3As_2 interface using soft point contact spectroscopy (PCS) measurement, which can push the tip-induced superconductivity from the point contact to the interface platform.

The Cd_3As_2 single crystals were grown using the vapor-phase self transport method. The source was polycrystalline Cd_3As_2, which was synthesized using a normal solid-state reaction. Stoichiometric quantities of high-purity (99.999%) cadmium and arsenic elements were mixed and vacuum sealed in a quartz tube. The tube was heated at 850 ℃ for 5 h and subsequently quenched in liquid nitrogen. The obtained polycrystalline Cd_3As_2 ingot was ground into powder and sealed in a quartz tube. This tube was incubated for two days in a two-zone furnace with a temperature gradient from 575 to 500 ℃ for two days and then naturally cooled down to room temperature. Single crystals having a typical size of $2 \times 2 \times 2\,\mathrm{mm}^3$ were collected at the low-temperature side.

Au and Pt films were deposited on the Cd_3As_2 single crystals using the AFS1300 magnetron sputtering system (Ace Precision Machine, Inc.). The thick-

Supported by the National Natural Science Foundation of China (Grant Nos. 11704403 and 11874417), the National Key Research Program of China (Grant Nos. 2016YFA0401000, 2016YFA0300604, and 2018YFA070112), and the Strategic Priority Research Program (B) of Chinese Academy of Sciences (Grant No. XDB33010100).

*Corresponding authors. Email: szhang@iphy.ac.cn; lshan@ahu.edu.cn; gfchen@iphy.ac.cn

© 2020 Chinese Physical Society and IOP Publishing Ltd

ness of the deposited film was controlled by adjusting the sputtering time and maintaining the remaining parameters (pressure, temperature, distance, and voltage) constant during the sputtering procedure. In the present study, magnetron sputtering for 10 min yielded an approximately 20-nm-thick Au/Pt film on the crystal surface. Throughout the sputtering process, the substrate was maintained at room temperature. All the crystals with deposited films were annealed at 200–300℃ for 3–6 h under one-bar pressure in the magnetron sputtering chamber. The PCS and ZBCR measurements were performed using a Quantum Design physical property measurement system (PPMS). To mimic a soft contact, a tiny drop of silver paint was deposited on the clean surface of the deposited thin film for connecting a conducting wire. The material of the leading wire (Ag, Au, or Pt wires with diameter of 15–25 μm) did not affect the results. The soft PCs were prepared at room temperature in an ambient atmosphere. The soft contact area was approximately $40 \times 40\,\mu m^2$.

The main experimental parameters that influence the soft PCS results include the deposited metal, crystal plane, annealing condition, thickness of the deposited film, and PC area. The interfacial superconductivity in the case of Pt and Au/Cd_3As_2 was successfully detected using the soft PC technique. All the observations were obtained on the naturally grown crystal face (112) of the Cd_3As_2 crystals. The annealing temperature was maintained at approximately 200 ℃ to avoid the occurrence of additional reactions.

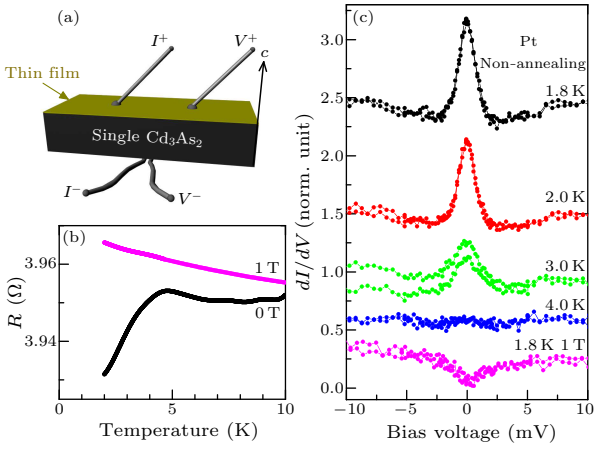

Fig. 1. (a) Schematic diagram of the PCS measurement configuration. (b) Temperature dependence of zero-bias contact resistance (ZBCR) in the presence and absence of a magnetic field perpendicular to the crystal surface. (c) The dI/dV spectra obtained when temperature increased from 1.8 to 4.0 K. The spectrum at 1.8 K under 1 T is shown for comparison. The sample was Pt-deposited Cd_3As_2 with no annealing treatment.

Figure 1(a) illustrates the soft PC configuration used in this study. One pair of current and voltage terminals (I^+ and V^+) was set on the surface of the deposited thin film, whereas the other pair (I^- and V^-) was connected at the bottom of the crystal to insure that the electric current flowed through the interface and crystal. Figure 1(b) shows the temperature-dependent ZBCR $R(T)$ of the Cd_3As_2 deposited with the Pt film. A clear but weak drop was observed at 4.8 K under no field. With a magnetic field of 1.0 T applied perpendicular to the surface, ZBCR $R(T)$ shows a linear-like temperature dependence. The corresponding PCS results are presented in Fig. 1(c). The spectra observed at temperatures lower than 4.0 K display a zero-bias conductance peak (ZBCP), which decays continuously and finally fades away with increasing temperature and magnetic field. Such a temperature- and magnetic field-dependent drop in ZBCR $R(T)$ and ZBCP can be attributed to the superconducting phase. The interfacial superconductivity induced using a thin film coating is consistent with the tip-induced superconductivity observed in previous PCS studies using the hard PC method.[1,8] The weak signal can be attributed to the weak coupling at the Pt/Cd_3As_2 interface, which may be caused by the deposition process without any further annealing treatment. Thus, the annealing is not a requisite experimental condition for the ZBCP but can significantly improve the signals, as discussed later.

Two typical spectra of the Cd_3As_2 deposited with Pt film and annealed at 200 ℃ are displayed (Figs. 2(a) and 2(b)) to understand the characteristics of the soft PCS results. As shown in Fig. 2(a), the spectra of sample A are dominated by a typical shape of the Andreev reflection with two symmetric peaks (±2 mV) flanking the central dip. The additional pairs of tiny dips at ±5.5 and ±8.5 mV could be attributed to the critical current effect that occurs in the multiple parallel channels of a large contact area. This effect is especially prominent in soft contact measurements.[4,9–11] Alternatively, the phenomenon of multiple conductance peaks can be related to the unconventional superconductivity. A similar set of double conductance peaks symmetric around zero bias has been observed on Cd_3As_2 via a hard PCS measurement, suggesting a p-wave-like unconventional superconductivity.[1] Figure 2(b) shows the spectra of another sample treated under identical experimental conditions, including deposition and annealing. The zero bias voltage was symmetrically flanked by two pairs of sharp dips, one at ±2.5 and the other at ±7 mV. As the temperature increased from 1.8 to 8.0 K, the spectra gradually weakened to a linearly trending dI/dV with no clear dips or peaks. Similarly, an external field application suppressed the spectra, as shown in Fig. 2(c). The broad V-shaped spectrum is considered as a background signal. The sample dependence of the obtained spectra may reflect the different contact conditions of the two samples because the film conditions of samples A and B should be almost identical. Thus, the contact resistance of samples A and B are 2.8 and 12.5 Ω,

respectively. Figure 2(d) shows the corresponding ZBCR $R(T)$'s of samples A and B, which are compared with the ZBCR data obtained from the PCS spectra in Figs. 2(a) and 2(b). The clear drop around 7.1 K corresponds to the superconducting transition, which completely suppressed the magnetic field by approximately 1.0 T. The superconducting component and transition temperature at the Pt/Cd_3As_2 interface were obviously more developed in the annealed samples than in the non-annealed sample (Fig. 1).

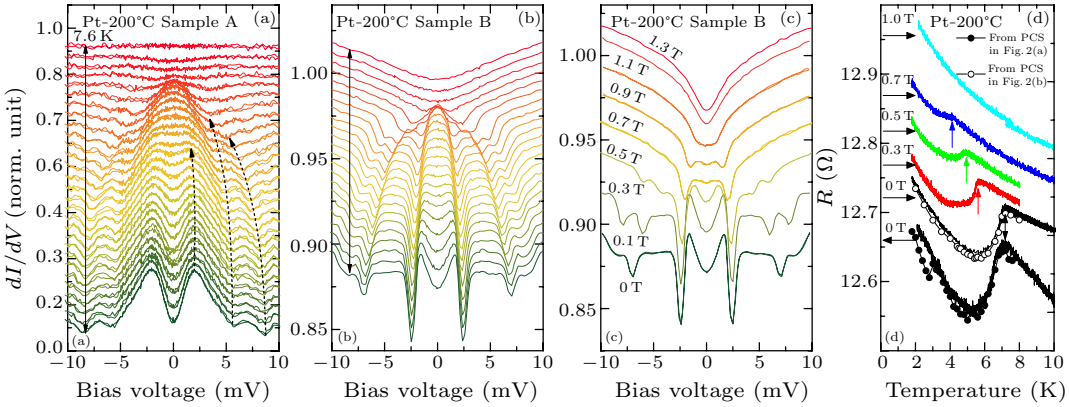

Fig. 2. The dI/dV spectra obtained at different temperatures: (a) sample A (Pt-200°C, 1.8–7.6 K at 0.2 K interval) and (b) sample B (Pt-200°C, 2.0, 2.5, 3.0, 3.5, 4.0, 4.4, 4.5, 4.6, 4.8, 5.0, 5.2, 5.4, 5.5, 5.6, 5.8, 6.0, 6.2, 6.6, 6.8, 7.0, 7.2, 7.5, and 8.0 K). (c) The dI/dV spectra of sample B (Pt-200°C) at 1.8 K, obtained as magnetic field increased from 0.1 to 1.3 T at 0.2 T intervals. (d) Temperature dependence of ZBCR $R(T)$ of samples A and B under different applied fields up to 1.0 T. The open (○) and solid (·) circles are the ZBCR data obtained from the PCS in Figs. 2(a) and 2(b), respectively.

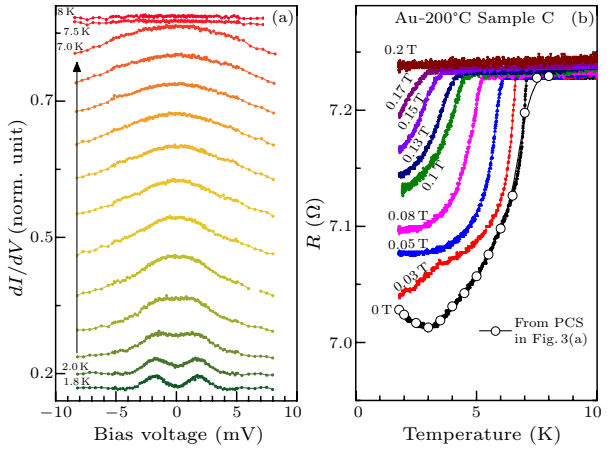

Fig. 3. (a) The dI/dV spectra of sample C (Au/Cd_3As_2) obtained at different temperatures (1.8–8.0 K at 0.5 K intervals). This sample was annealed at 200℃. (b) Temperature dependence of ZBCR $R(T)$ of sample C under different magnetic fields up to 0.2 T. The open circles (○) are the ZBCR data obtained from the PCS in Fig. 3(a).

Figure 3(a) denotes the PCS measurements of the Au/Cd_3As_2 interfaces exhibiting the similar spectra, where the Au deposited crystals were annealed at 200℃ (sample C). The weak but clean dip with symmetrical peaks, which can be observed at ±2 mV, is considered to be the Andreev reflection spectrum. As the temperature increased from 1.8 to 3 K, the central dip transformed into a broad hump, persisting from 3.0 to 7.0 K. In the corresponding plot of ZBCR versus temperature (Fig. 3(b)), $R(T)$ suddenly dropped at 7.1 K. This transition temperature and the Andreev reflection-type spectra are common characteristics of the Pt and Au/Cd_3As_2 interfaces annealed at 200℃. However, the huge difference between the upper critical magnetic fields of Pt and Au/Cd_3As_2 (1.0 T and as low as 0.2 T, respectively) remains unexplained.

Heating treatments for the Au-deposited Cd_3As_2 were extensively performed at 200 and 230 ℃. Figures 4(a) and 4(b) show the PCS of sample D annealed at 230℃ based on the scanning temperature and magnetic field, respectively. The spectra are dominated by a broad ZBCP flanked by deep and symmetric dips at ±5 mV. A small cap-like ZBCP can be observed in the PC spectrum at temperatures of lower than 2.6 K, although it is difficult to discuss the correlation between the small ZBCP and the main feature. A similar minor ZBCP character has been reported for double conductance peaks related to an unconventional superconducting mechanism.[1]

The ZBCR $R(T)$ exhibits a steep drop at 3.8 K, which is gradually suppressed as the magnetic field increased to 0.25 T, as shown in Fig. 4(c). Samples C and D differ only with the respect to their annealing temperatures (200℃ and 230℃, respectively). However, they yielded distinct PCS spectra and transition temperature T_c's. Furthermore, it appears that the interfacial superconducting state with the lower T_c (3.8 K) displays an $H_{c2} \sim 0.25$ T, which is slightly larger than the value of 0.2 T observed when T_c = 7.1 K. The T_c and H_{c2} values obtained in this study are summarized in Fig. 4(d). The Pt and Au/Cd_3As_2 interfaces exhibits the same T_c value. However, their H_{c2} values were considerably different. Because superconductivity was observed on the non-annealed Pt/Cd_3As_2 interface, we can conclude that the heating treatment at suitable temperatures improved the superconducting features.

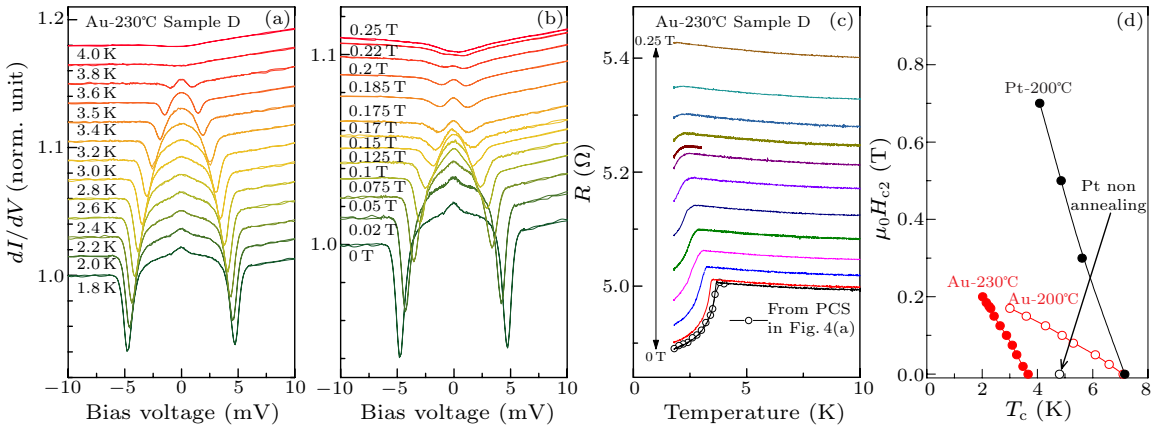

Fig. 4. (a) The dI/dV spectra of sample D (Au/Cd_3As_2) collected at different temperatures (1.8–4.0 K at 0.2 K intervals). The sample is annealed at 230 °C. (b) The dI/dV spectra at 1.8 K and (c) temperature dependence of ZBCR $R(T)$, obtained under different applied fields (0–0.25 T at 25 mT intervals). The open circles (○) are the ZBCR data obtained from the PCS in Fig. 4(a). (d) Summarized H–T phase diagram of four typical samples.

Although the complex spectral features barely fitted with the two-channel Blonder–Tinkham–Klapwijk (BTK) model,[12–14] the superconducting gap Δ could be approximately estimated from the symmetric peak/dip positions. The estimated Δ values are 1.6–2.0 mV for the Pt and Au/Cd_3As_2 interfaces, similar to those reported Δ in hard PC-induced superconductivity study.[8] We consider the following situation to interpret the different H_{c2} values. The thin films deposited on the Cd_3As_2 crystal surface are not atomically uniform and flat because of the technical characteristics of magnetron sputtering; instead, they form many small-area islands responsible for the superconducting transitions. The non-superconducting components connecting these interfacial islands are easily penetrated by magnetic fluxes. However, more evidence is required to clarify the intrinsic mechanism of the different H_{c2}. The superconducting state probed in the PCS measurements is dominantly determined by the number and features of the interfacial islands under the soft contact of silver paint. Improving the quality of the interface would probably elicit bulk-like superconductivity behavior, including zero electrical resistance and diamagnetism. This assumption is currently being investigated. Here, all our obtained T_c values differed from the sub-kelvin superconducting transition temperature recently observed in the case of the Cd_3As_2 thin films.[15]

In summary, we have observed the interfacial superconductivity on the 3D Dirac semimetal Cd_3As_2. The interfacial superconductivity is considerably dependent on the deposited metal, annealing treatment and specific point contact condition, as also reported for the hard PC-induced superconductivity. After reproducing the local superconductivity on normal metal-coated Cd_3As_2, we can conclude that the pressure effect around the tip contact makes a minor contribution to the induced superconductivity. The mechanism by which superconductivity appears on topological materials must be clarified using other typical examples.

References

[1] Wang H, Wang H, Liu H, Lu H, Yang W, Jia S, Liu X J, Xie X C, Wei J and Wang J 2016 *Nat. Mater.* **15** 38

[2] Aggarwal L, Gayen S, Das S, Kumar R, Süß V, Felser C, Shekhar C and Sheet G 2017 *Nat. Commun.* **8** 13974

[3] Wang H, Wang H, Chen Y, Luo J, Yuan Z, Liu J, Wang Y, Jia S, Liu X J, Wei J and Wang J 2017 *Sci. Bull.* **62** 425

[4] Hou X y, Wang Z, Gu Y d, He J b, Chen D, Zhu W l, Zhang M d, Zhang F, Xu Y f, Zhang S, Yang H x, Ren Z a, Weng H m, Hao N, Lv W g, Hu J p, Chen G f and Shan L 2019 *Phys. Rev. B* **100** 235109

[5] Aggarwal L, Singh C K, Aslam M, Singha R, Pariari A, Gayen S, Kabir M, Mandal P and Sheet G 2019 *J. Phys.: Condens. Matter* **31** 485707

[6] Wang H, Ma L and Wang J 2018 *Sci. Bull.* **63** 1141

[7] Zhu W, Hou X, Li J, Huang Y, Zhang S, He J, Chen D, Wang Y, Dong Q, Zhang M, Yang H, Ren Z, Hu J, Shan L and Chen G 2020 *Adv. Mater.* **32** 1907970

[8] Aggarwal L, Gaurav A, Thakur G S, Haque Z, Ganguli A K and Sheet G 2016 *Nat. Mater.* **15** 32

[9] Bugoslavsky Y, Miyoshi Y, Perkins G K, Caplin A D, Cohen L F, Pogrebnyakov A V and Xi X X 2004 *Phys. Rev. B* **69** 132508

[10] Miyoshi Y, Bugoslavsky Y and Cohen L F 2005 *Phys. Rev. B* **72** 012502

[11] Shan L, Huang Y, Ren C and Wen H H 2006 *Phys. Rev. B* **73** 134508

[12] Blonder G E, Tinkham M and Klapwijk T M 1982 *Phys. Rev. B* **25** 4515

[13] Dynes R C, Garno J P, Hertel G B and Orlando T P 1984 *Phys. Rev. Lett.* **53**(25) 2437

[14] Tanaka Y and Kashiwaya S 1995 *Phys. Rev. Lett.* **74** 3451

[15] Suslov A V, Davydov A B, Oveshnikov L N, Morgun L A, Kugel K I, Zakhvalinskii V S, Pilyuk E A, Kochura A V, Kuzmenko A P, Pudalov V M and Aronzon B A 2019 *Phys. Rev. B* **99** 094512